Spatial distribution of water and wind erosion and their influence on the soil quality at the agropastoral ecotone of North China

International Soil and Water Conservation Research 8 (2020) 253–265

Contents lists available at ScienceDirect

International Soil and Water Conservation Research

journal homepage: www.elsevier.com/locate/iswcr

Original Research Article

Spatial distribution of water and wind erosion and their influence on the soil quality at the agropastoral ecotone of North China

Yanzai Wang [c], Yifan Dong [a, *], Zhengan Su [b], Simon M. Mudd [d], Qiuhong Zheng [e], Gang Hu [f], Dong Yan [g]

[a] Institute of International Rivers and Eco-Security, Yunnan University, Kunming, 650091, PR China
[b] Key Laboratory of Mountain Hazards& Surface Process, Institute of Mountain Hazards and Environment, Chinese Academy of Sciences, Chengdu, 610041, PR China
[c] College of Geography and Tourism, Chongqing Normal University, Chongqing, 401331, PR China
[d] School of GeoSciences, University of Edinburgh, Edinburgh, EH8 9XP, UK
[e] China Meteorological Administration Training Center, CMA, Beijing, 100081, PR China
[f] School of Tourism and Geography Sciences, Qingdao, 266071, Shandong, PR China
[g] National Institute for Radiological Protection, Chinese Center for Disease Control and Prevention, Beijing, 100088, PR China

ARTICLE INFO

Article history:
Received 29 July 2019
Received in revised form
10 April 2020
Accepted 6 May 2020
Available online 18 May 2020

Keywords:
Soil erosion
Soil quality
Spatial distribution
Agropastoral ecotone

abstract:

In semiarid regions, wind and water erosion are serious environmental and ecological problems around world. They have different impacts on soil quality over a range of spatial scales. Analyzing the spatial distribution of soil erosion and understanding the impacts of wind and water erosion on soil quality at the regional scale is vital for mitigating soil erosion risk. In this study we explore the spatial distributions of water and wind erosion around Zhangjiakou city which suffers both water and wind erosion contemporaneously, and detect the influence of soil erosion on soil quality. We find that annual wind erosion intensities range 4.99–10.05 t ha^{-1} yr^{-1}, and annual water erosion intensities range 2.92–4.14 t ha^{-1} yr^{-1}. Areas with higher potential wind and total erosion risk occur mainly in northwest and southeast Zhangjiakou city, whereas potential water erosion risk is highest in the southwest and central regions. The highest erosion rates are concentrated in gentle parts of the landscape, where agriculture has led to low vegetation cover. Steeper portions of the landscape, which remain forested, have lower erosion rates. These spatial patterns are dominated by higher wind erosion, which correlates with surface soil coarsening and higher water infiltration, whereas the soil water holding capacity decreases with increasing wind erosion rates. In regions with high water infiltration rates, we find the intensity of water erosion weakened. To mitigate risks of soil degradation, suitable erosion measures should be implemented according to the dominant erosion type, which varies in space.

1. Introduction

Accelerated soil erosion has numerous environmental and ecological effects. Where soil erosion occurs, it leads to deterioration of soil health because it degrades soil quality and disrupts both mechanical and chemical processes in the soil (Lal, 2001). Eroded soil can result in sedimentation of reservoirs and waterways, non-point source pollution, emission of greenhouse gases and a decline in the quality of both water and air (Lal, 2018; Shi, Yan, Yuan, & Nearing, 2004).

Soil and nutrient losses are dominated by water and wind erosion (e.g., Tuo, Xu, & Gao, 2018). In semiarid regions, wind and water erosion may occur contemporaneously (Du, Dou, Deng, Xue, & Wang, 2016; Tuo, Xu, Zhao, & Gao, 2015; Van Pelt et al., 2017; Visser, Sterk, & Ribolzi, 2004; Zhang et al., 2011b). Visser et al. (2004) argued that to better understand the impact of wind and rainfall on soil degradation in semi-arid areas, processes should be studied simultaneously. Despite the potential importance of mechanisms of erosion in dryland environments, limited studies have quantified the absolute and relative magnitudes of wind and water erosion at the same site over the same time period

* Corresponding author.
E-mail address: yifan@ynu.edu.cn (Y. Dong).

https://doi.org/10.1016/j.iswcr.2020.05.001

(Breshears, Whicker, Johansen, & Pinder, 2003). Tuo et al. (2015) argued that effective mitigation of erosion risk requires controls of water and wind erosion because the two mechanisms amplify each other. A key factor in the effectiveness of these measures is coeval assessment of wind and water erosion.

To understand appropriate mitigation strategies for soil erosion, one must determine the relative influence of water and wind, which varies between regions. Soil erosion is a scale-dependent phenomenon, the small-scale and large-scale effects on the soil quality can vary widely (Berhe, Barnes, Six, & Marín-Spiotta, 2018; Lal, 2001). Zhang et al. (2011b) reported that the soil erosion rate caused by the combined effects of water and wind in southern Arizona was 7.60 t ha^{-1} yr^{-1}, although wind was responsible for only 0.08 t ha^{-1} yr^{-1}. Van Pelt et al. (2017) reported that wind erosion was responsible for about 75% of the total soil loss in semiarid regions of the USA. Tuo et al. (2018) recently reported the contributions of water and wind erosion in Chinese Loess Plateau were different on slopes with different aspect, different gradient, and different soil physical and chemical properties. These variations also modulated the total soil erosion.

As for the impact of soil erosion on soil nutrients, Visser, Stroosnijder, and Chardon (2005) observed that nutrient losses by water erosion were small compared with those by wind erosion in the Sahelian zone of West-Africa. This small contribution, however, could have serious impacts to soil health because nutrients lost by water were permanently transported away from the area. In addition, Visser et al. (2005) found that sediment transport by wind in which grains were saltating resulted in the largest soil and nutrient loss on the event timescale. Subsequently, Visser and Sterk (2007) found that water and wind erosion had different impacts on nutrient losses when looking at different spatial scales: the nutrient losses caused by soil erosion at the village scale were considerably smaller than at the plot scale. However, the impacts of water and wind erosion on soil nutrients at the regional scale, and how the water and wind erosion affected other soil qualities such as soil texture have not been reported in past studies.

Numerous studies have documented the soil erosion risk in semiarid China (Fu et al., 2011; Shi et al., 2004; Wei, Chen, Fu, Lü, & Gong, 2009). These authors predominantly studied wind and water erosion as two separate processes. Meanwhile, most studies featuring combined assessments of water and wind erosion in China have focused on the Loess Plateau and Inner Mongolia (Du et al., 2016; Jiang, Zhang, Zhang, & Wang, 2019; Tuo et al., 2015, 2018), due to the regions' importance for agricultural production. However, the semiarid regions north of Beijing, of which the Zhangjiakou city area is one, have received little attention. Zhangjiakou city sits at the boundary of Inner Mongolia, which experiences severe wind erosion region (Zhang et al., 2018), and the Loess Plateau, which experiences severe water erosion (Fu et al., 2011). We anticipate strong spatial variations in the relative magnitude of these two erosion mechanisms around Zhangjiakou city, making it an ideal site to explore the relative impacts of water and wind erosion. In addition, the expected intensive land use changes associated with the 2022 Olympic Games means it is imperative to assess the soil erosion potential risk and discuss its influence on the regional environment (Cyranoski, 2015.; Liu et al., 2018; Song et al., 2018).

Zhang, Yang, Pan, and Zhang (2011a) have calculated the wind erosion rate of farm land in the north region of Zhangjiakou city using the ^{137}Cs tracer technique, and calculated an average rate of 89.5 t ha^{-1} yr^{-1}. However, Zhang, Zhang, Chang, Wang, and Liu (2017) recently reported that the wind erosion rate of farm land in the same area was lower, from 40.1 t ha^{-1} yr^{-1} to 47.9 t ha^{-1} yr^{-1} using SWEEP model (Zhang et al., 2017). In general, these assessments of wind erosion did not cover the whole area of Zhangjiakou city. Meanwhile, water erosion in Zhangjiakou city has not been reported previously. Furthermore, Zhang et al. (2011a) found that surface soils of farmland in Zhangjiakou city became coarser because of wind erosion, the proportion of sand particles larger than 0.05 mm exceeded 67% in the plough layer and higher than that in grasslands. However, the impact of soil erosion in Zhangjiakou city on other soil quality parameters such as soil nutrients (e.g., organic carbon and nitrogen) was not quantified, even though these parameters would affect the soil nutrient availability and ecosystem's provisioning service (Bilotta, Grove, & Mudd, 2012).

In this study, we use soil erosion models and ^{137}Cs inventories to estimate annual water and wind erosion intensity and long-term soil erosion, respectively. We also detect the influence of soil erosion on soil quality such as soil grain size, soil hydraulic and soil nutrient indices in Zhangjiakou city. The objectives of this study are (a) to explore the spatial distribution of water and wind erosion intensity in Zhangjiakou city, and quantify the contributions to total erosion over the whole study area; (b) to reveal the influences of soil erosion on various parameters of soil quality on regional scales.

2. Materials and methods

2.1. Study area

Zhangjiakou city is a prefectural level city (i.e., a regional administrative unit including both urbanized and non-urbanized areas) situated in the northwest of the Hebei province, China, bordering Beijing to the southwest, Inner Mongolia to the north and northwest, and the Loess Plateau to the southwest (Fig. 1a). The main construction efforts for the 2022 Olympic venues and supporting facilities will occur in Chongli, which is a small county in central Zhangjiakou city (Fig. 1b–c) (Song et al., 2018).

Zhangjiakou city has a continental monsoon climate, with high annual temperature variation, and less rainfall (Table 1). The dominant wind direction in Zhangjiakou is from northwest to southeast. Gales, defined as wind speeds higher than 17 m s^{-1}, mostly occur in the northern part of Zhangjiakou city between March and May (Zhang et al., 2011a). Zhangjiakou city lies at the transition zone between the Inner Mongolia Plateau and the North China Plain (Fig. 1b,d). The elevation has a general trend of increasing elevations from southeast to northwest. Zhangjiakou city can be classified into three different geomorphic units, each one of them has different landform characteristics (Table 1). Zhangjiakou city itself belongs to the agropastoral ecotone, grass, forestry and arable land are the main land use types (Fig. 1e–f).

2.2. Data preparation and statistical analysis

(1) modelling data preprocess

In this study, DEM (Digital elevation model) data, land use data, NDVI (Normalized difference vegetation index) data, and two types of daily meteorological data (gridded data of daily precipitation, and daily wind speed data) were used to assess water and wind annual erosion rates in Zhangjiakou city. The meteorological data from weather stations were interpolated into raster data with spatial resolution of 60 m using Kriging method. We resampled all spatial data with non-60 spatial resolution into grid pixels with a spatial resolution of 60 m. To assess the total erosion rate in decade scale, ^{137}Cs data in southern Zhangjiakou city was collected from Zhao, Yan, Zhang, Zhan, and Hu (2012) (Fig. 1i). Details of ^{137}Cs data collection and preparation follow standard procedures but details can be found in Zhao et al. (2012).

(2) field sampling and laboratory test of soil quality data

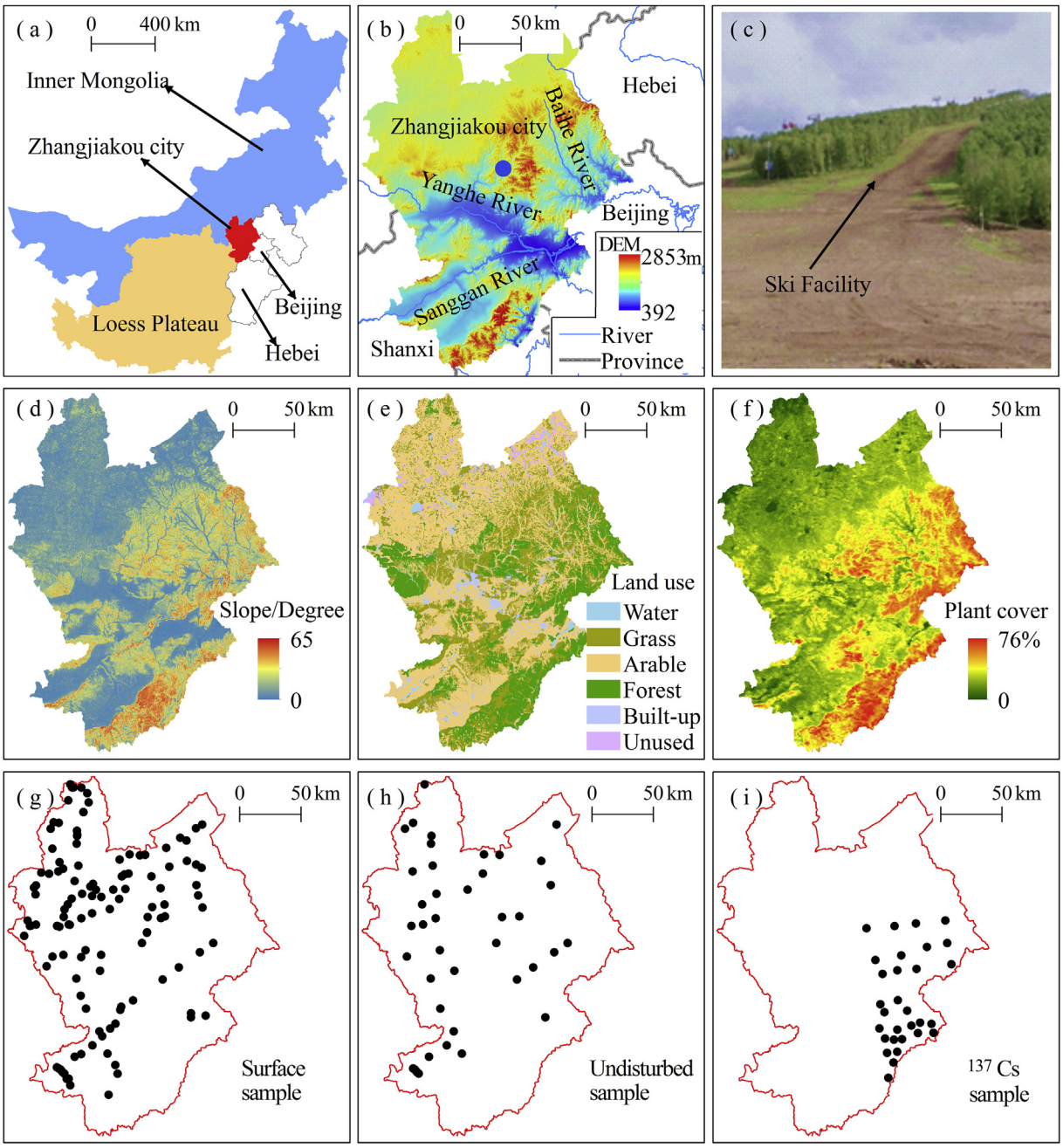

Fig. 1. The study area and the sampling sites of soil quality data.

Table 1
The geographic characteristics in Zhangjiakou city.

	Characteristics Description	
Climate	Temperature	average annual value:6.9 °C; the highest monthly value:22.4 °C; the lowest monthly value: 11.4 °C;
	Precipitation	average annual value:393.4 mm; 93.2% happens from April to October
	Wind	the dominant direction: from northwest to southeast; 66.3% of daily maximum wind speed >5.5 m s^{-1}
Landforms	Elevation	ranges from 392 m to 2853 m above sea level, with an increasing trend from southeast to northwest
	Slope	the average slope:9.8°; more than 24.2% of land area> 5°
	River	Yanghe River and Sanggan River cross Zhangjiakou city
	Geomorphic units (Yuan, Niu, & Wang, 2006)	eastern part: mountainous region with a steeper slopes; southwest part: a part of Loess Plateau, is comprised of alluvial and diluvial plain, loess hill and fringe mountains; northwest part: a part of Inner Mongolia Plateau, with an elevation 1000–1700 m and very low gradients.
Land use	Forest	are dominated by temperate broad-leaved deciduous species (Yuan et al., 2006)
	Grassland	are various species of shrubs, perennial and annual herbaceous plants
	Arable land	are mainly located in the region with gentle gradients

128 surface soil samples and 42 undisturbed soil samples were collected in the study area in June of 2018 (Fig. 1g–h). The collection depth of surface samples were 0–5 cm, and each sample has a weight about 1 kg. Undisturbed soil samples were collected by cutting ring, with a height of 5 cm, and a volume of 100 cm^3.

Two soil quality parameters that are of primary interest with regard to ecosystem services are soil texture and nutrient availability (Bilotta et al., 2012). In this study, particle size distribution data (PSD, unit: %), field capacity of soil moisture (unit: %), soil saturated hydraulic conductivity (K_s, unit: cm h^{-1}). Soil organic carbon (SOC, unit: g kg^{-1}) and total nitrogen (N, unit: g kg^{-1}) were chosen as soil quality parameters. The particle size distributions (PSDs) in this study were analyzed using the EOF method to extract the sensitive grain size fraction (GSF) (Wang, Wu, Lu, & Pan, 2018c). We found that the sensitive grain size fraction here is > 0.099 mm. Hence, for particle size, we performed the regression the content of GSF >0.099 mm and the total soil erosion in 2015. After surface samples were dried naturally, gravels were removed using a 2 mm aperture sieve. The remaining samples were used to measure PSD, SOC and N. PSD data of surface soil was measured using Malvern Mastersizer 2000 Particle size Analyzer in the School of Geography, Southwest University, China. SOC and N were measured using elemental analyzer (Elementar, Vario Max CN, Germany) in Institute of Mountain Hazards and Environment, Chinese Academy of Sciences (Li et al., 2017a). Undisturbed soil samples were used to measure field capacity of soil moisture and K_s. The field capacity of soil moisture was measured using the centrifugation method, and soil saturated hydraulic conductivity was tested using the constant head method (Wang, Shao, Han, & Liu, 2015), The field capacity of soil moisture and K_s were measured in the College of Urban & Environmental Sciences, Central China Normal University.

(3) data statistics analysis method

After soil erosion calculation, we classified soil erosion intensity following the scheme of Du et al. (2016), and extracted the land area fraction within Zhangjiakou city for each soil erosion intensity (Table 2). In addition, to better understand the spatial distribution of water and wind erosion, we compiled the water and wind erosion intensities in terms of environmental and anthropogenic factors.

After laboratory test of soil samples, we spatially interpolated data of each soil quality parameter into a raster format using the kriging method. Following the method introduced by Jiang et al. (2019), the value range of each soil quality parameter was divided into twenty intervals, and we extracted the average value for each interval and its corresponding estimated soil erosion in 2015. Finally, we used regression to explore whether the measured soil quality parameters were correlated with predicted erosion rates or not. In addition, the relationships between soil erosion and soil quality would be strongly affected by land use type, thus, we performed the regression analysis between soil erosion and soil quality for arable land and non-arable land, respectively.

Table 2
The land area proportion of different soil erosion intensity.

Soil erosion intensity/t ha^{-1} yr^{-1}	Water erosion			Wind erosion		
	2005	2010	2015	2005	2010	2015
<2.0	**64.7**	**53.6**	**54.0**	**37.6**	**26.6**	**45.2**
2.0–25.0	33.3	43.8	43.3	**58.7**	**63.5**	**54.8**
25.0–50.0	1.7	2.2	2.4	3.6	10.0	0
50.0–80.0	0.3	0.3	0.3	0	0	0
80.0–150.0	0.1	0.1	0	0	0	0
>150.0	0	0	0	0	0	0

The unit of land area proportion is: %.

2.3. Water erosion assessment

A number of methods have been used to model water erosion over areas with mixed land use. The USLE (The universal soil loss equation) and RUSLE (The revised universal soil loss equation) are amongst the most frequently used due to several advantages: simple modelling processes; fewer input parameters; and well tested predictions (e.g., Aksoy & Kavvas, 2005; Jiang et al., 2019; Tuo et al., 2018). The USLE model has been applied in estimation soil erosion for many regions worldwide (e.g., Aksoy & Kavvas, 2005), frequently supported by GISand remote sensing (e.g., Fu et al., 2011). Ongoing improvements have been made for the calculation of various factors of USLE based on the erosion environment for specific regions: a number of authors have developed local USLE factors in the semiarid regions of China (Fu et al., 2011; Jiang et al., 2019; Nearing, Xie, Liu, & Ye, 2017).

In this study, we used a modified version of the USLE model to calculate water erosion. It can be defined as follows (Wischmeier & Smith, 1978):

$$A = R \times K \times LS \times C \times P \tag{1}$$

Where A is the calculated water erosion rate (t ha^{-1} yr^{-1}); R is the rainfall-runoff erosivity factor (MJ mm $ha^{-1}\cdot h^{-1}\cdot yr^{-1}$); K is the soil erodibility factor (t h $MJ^{-1}\cdot mm^{-1}$); LS is the slope-length and steepness factor, dimensionless; C is the cover management factor, dimensionless; and P is the conservation support practice factor, dimensionless.

The rainfall-runoff erosivity factor, R, is an indicator of the potential that precipitation will detach and transport soil particles (Teng et al., 2018). In this study, gridded daily rainfall data was used to calculate R using the power function model of (Zhang et al., 2003), which they successfully tested against field data in northern China and which has been used successfully in subsequent studies (Wu et al., 2018).

$$R_i = \alpha \sum_{j=1}^{k} \left(d_j^i\right)^{\beta} \tag{2}$$

where R_i is the i half-month value (MJ mm ha^{-1} h^{-1}); k is the number of days in the i half-month; and d_j^i is the erosive rainfall for j day of the i half-month, which is ≥12 mm. The parameters α and β are calculated with:

$$\alpha = 21.586 \times \beta^{-7.1891} \tag{3}$$

$$\beta = 0.8363 + \frac{18.114}{d_{12}} + \frac{24.455}{y_{12}} \tag{4}$$

where d_{12} is the average daily erosive rainfall (mm), y_{12} is the average annual erosive rainfall (mm). Annual rainfall erosivity, R, is the total rainfall erosivity within a year, can be aggregated by summing all half-month $R_i$values in the year.

The soil erodibility factor, K, describes the vulnerability of the soil to raindrop detachment and runoff wash (Fu et al., 2011). In this study, the K factor data was derived from Gao et al. (2012). They calculated K factor values using a soil erodibility nomograph which estimated the erodibility at a specific site by analyzing soil condition and soil types (Efthimiou, 2018; Liu, Bi, & Fu, 2010; Wischmeier & Smith, 1978).

Topographical factors, such as slope length and steepness, substantially affect the rate of water erosion (Liu, Nearing, & Risse, 1994; Visser et al., 2004; Wischmeier & Smith, 1978). In this

study, two topographic factors, slope length factor L and slope steepness factor S are calculated with (Liu et al., 1994; Renard et al., 1997):

$$L = (\lambda/22.1)^{m} \quad (5)$$

$$S = 10.8\ sin\theta + 0.03 \qquad \theta < 5^0 \quad (6)$$

$$S = 16.8\ sin\theta - 0.50 \qquad 10^0 > \theta \geq 5^0 \quad (7)$$

$$S = 21.9 sin\theta - 0.96 \qquad \theta \geq 10^0 \quad (8)$$

where λ is the slope length (m) measured along a horizontal projection, m is a variable slope length exponent which is related to the ratio, $\overline{\beta}$, of rill erosion to inter-rill erosion, and θ is the slope angle.

The variable slope-length exponent$m$ and the ratio $\overline{\beta}$ of rill erosion to inter-rill erosion is computed using the following equations:

$$m = \overline{\beta}/(1+\overline{\beta}) \quad (9)$$

$$\overline{\beta} = (sin\theta / 0.0896) \Big/ \left[3(sin\theta)^{0.8} + 0.56\right] \quad (10)$$

The cover and management factor C in the USLE measures the combined effect of all interrelated cover and management variables (Wischmeier & Smith, 1978). Previous studies developed a series of methods to estimate the C factor value using vegetation cover based on simulated and natural rainfall on experimental plots (Fu et al., 2011). In this study, we calculate C with the following (Jiang, Wang, & Liu, 1996; Liu et al., 2010):

$$C = e^{-0.0418(vc-5)} \quad (11)$$

$$C = 0.988\ e^{-0.11vc} \quad (12)$$

$$C = 1.029e^{-0.0235vc} \quad (13)$$

Eq. (11) is applied to grassland (Jiang et al., 1996) and Eq. (12) is applied to forests (Liu et al., 2010). As for arable land, considering the monthly change in effectiveness of crop cover within the crop year, the C factor of arable land was evaluated using Eq. (11), Eq. (12) and Eq. (13) for three different crop stage periods, a stage from April to June, a stage from July to September, and a stage of October to March in the following year, respectively (Liu et al., 2010). The annual C value was calculated using a weighted mean with the monthly rainfall erosivity as the weights.

Vegetation coverage (vc,%) was calculated using $NDVI$ data (Fu et al., 2011).

$$vc = \frac{(NDVI - NDVI_{soil})}{(NDVI_{max} - NDVI_{soil})} \quad (14)$$

where $NDVI_{soil}$ is $NDVI$ of bare soil; $NDVI_{max}$ stands for regional maximum $NDVI$. We obtained NDVI data from the Chinese Academy of Sciences.

The factor P is the ratio of soil loss with a specific cropping practice to the corresponding loss with cropping that is perpendicular to topographic contours (i.e., up-and-down cropping) (Wischmeier & Smith, 1978). At large spatial scales, it is difficult to capture the effects of soil and water conservation measures (such as terrace systems, contour tillage and strip-cropping on the contour) with land use maps (Fu et al., 2011). A recent study found the soil loss ratio, P, is greater with greater topographic gradient (Zhao, Yang, & Govers, 2019). In addition, the practice of narrow strip-cropping using a strips of approximately 2 m width has frequently been used in Zhangjiakou city (Fig. 2) as an erosion mitigation measure on slopes with topographic gradients greater than 0.27 (i.e., >15°). In these areas we calculated the P factor using annual rainfall data. Given the above considerations, two statistical formulas were used to determine the value of the P:

$$P = 0.2 + 0.03\overline{\theta} \qquad \overline{\theta} \leq 27 \quad (15)$$

$$P = 0.0039 \times y_{20}^{0.6772} \qquad \overline{\theta} > 27 \quad (16)$$

where $\overline{\theta}$ is the slope gradient in %, calculated directly from the DEM data. y_{20} is sum of the daily rainfall above > 20 mm over the whole year (an integer value that represents then number of days).

2.4. Wind erosion assessment

We used a statistical wind erosion equation to estimate the wind erosion rate in Zhangjiakou city. The equation was developed for semiarid environments using wind tunnel experiments and field observations (Gao et al., 2012). The equation has been applied to estimate wind erosion rates and dust emissions in previous studies; it was expressed using the following:

$$Q_1 = 10 \cdot \widehat{C} \cdot \sum_{j=1} < T_j \cdot exp\left\{ a_1 + \frac{b_1}{z_0} + c_1 \cdot \left[(A \cdot u_j)^{\frac{1}{2}} \right] \right\} > \quad (17)$$

$$Q_2 = 10 \cdot \widehat{C} \cdot \sum_{j=1} < T_j \cdot exp\left\{ a_2 + b_2 \cdot vc^2 + \frac{c_2}{A \cdot u_j^{'}} \right\} > \quad (18)$$

where, Q_1 (t ha^{-1} yr^{-1}) is the wind erosion rate in arable land with no vegetation cover; Q_2 (t ha^{-1} yr^{-1}) is the wind erosion rate in areas with plant cover, t ha^{-1} yr^{-1}; $\widehat{C}$ is a scaling parameter that in our sites is 0.0018; T_j is the accumulated time of wind speed $u_j(u_j^{'})$, minute; A is a conversion parameter of wind speed between field stations and data derived from wind tunnels, which in our study is 0.893; z_0 is the aerodynamic roughness length, here is 0.55 cm; vc is the plant coverage (%); other parameters a_1 and a_2, b_1 and b_2, c_1 and c_2 are −9.208 and 2.4869, 0.018 and −0.0014, 1.955 and −54.9472; u_j is station wind speed greater than sand particle's threshold wind under lower plant coverage, here the threshold wind speed is 5.5 m s^{-1}; $u_j^{'}$ is station wind speed greater than sand particle's threshold wind with plant coverage. According to wind tunnel experiments, the threshold wind speed u_t can be expressed as a function of plant coverage:

$$u_t = = 5.56158 + 1.63299 \times \exp\left(\frac{vc}{38.6747}\right) \quad (19)$$

We used Eq. (18) To compute the wind erosion rate for grassland and forests. Because crop cover that is present before harvesting is effective in reducing wind erosion, we also use Eq. (18) For arable land in the crop-stage periods between April and September. In contrast, we use Eq. (17) To calculate the wind erosion rate for arable land during other periods of the year.

2.5. Total erosion assessment

In previous studies, total soil erosion was defined as the sum of water and wind erosion (Du et al., 2016; Jiang et al., 2019), meanwhile, the Cesium-137 (^{137}Cs) tracing technique was also used to estimate total soil erosion (Tuo et al., 2018; Van Pelt et al., 2017). In

Fig. 2. Soil erosion control practices in Zhangjiakou city.

this study, we use both of these methods to calculate total soil erosion in Zhangjiakou city, and we test these two predictions against each other.

In this study, we synthesized published ^{137}Cs inventories data in northern China and their corresponding soil erosion rate data (Li, Li, Liu, & Yao, 2005; bib_Qi_et_al_2008·Qi, Liu, Shi, Hu, & Zhuang, 2008; Yan et al., 2000, 2003·bib_Yan_et_al_2000·bib_Yan_et_al_2003; Zhang et al., 2007a). Deposition of ^{137}Cs is not homogenous in space and time, so we normalize the different ^{137}Cs inventories with a reference inventory (i.e., we divide ^{137}Cs values at each site with their local reference inventory). Our results are not sensitive to the selected reference inventory, but we selected the inventory from the site closest to our field site. reference ^{137}Cs inventory we use in the results presented here is 1602.79 Bq m^{-2} (Qi et al., 2008) and divided all ^{137}Cs inventories in our dataset to create a standardized inventory across all sites. We then regressed the standardized ^{137}Cs inventories against measured soil erosion rates using a variety of regressions (linear, logarithmic, polynomial) and found that the relationship between total soil erosion rate in northern China and standardized ^{137}Cs inventories is best described by a logarithmic relationship (Fig. 3).

We then aggregated the ^{137}Cs inventory data in southern Zhangjiakou city, which have been published in (Zhao et al., 2012). From these data, we employed the logarithmic regression formula to compute the total soil erosion in southern Zhangjiakou city, and described the spatial distribution of the total erosion rate inferred from ^{137}Cs inventories in the decade scale.

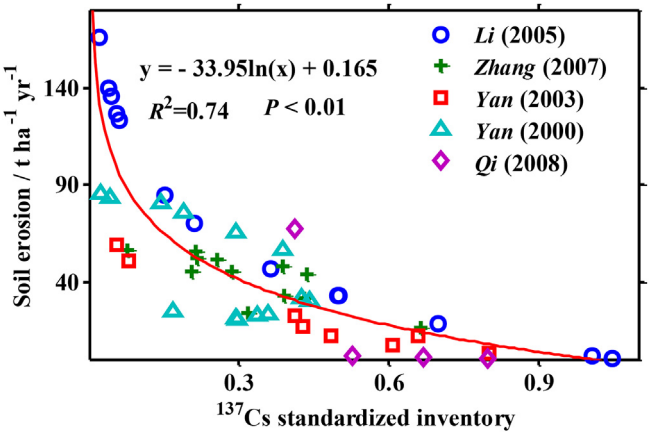

Fig. 3. The relationship between ^{137}Cs standardized inventories and soil erosion rate.

3. Results

3.1. Water and wind erosion

In Zhangjiakou city, our modelling predicts that annual water erosion rates are 2.9, 3.9, and 4.1 t ha^{-1} yr^{-1}, respectively for the years 2005, 2010 and 2015. We calculate annual wind erosion rates of 7.5, 10.1, and 5.0 t ha^{-1} yr^{-1} in the same years (Fig. 4), suggesting that the wind erosion rate exceeds the water erosion rate in Zhangjiakou city for each year. In addition, we find that the wind erosion in Zhangjiakou city peaks in 2010 and is twice of the value in 2015. The changing trend of wind erosion in Zhangjiakou city is similar to assessments of wind erosion in Inner Mongolia which lies on the north of Zhangjiakou city (Zhang et al., 2018). They reported that the wind erosion rates were 23, 42 and 23 t ha^{-1} yr^{-1}, respectively for 2005, 2010 and 2015.

We found that the fraction of land area experiencing erosion intensity <2 t ha^{-1} yr^{-1} in Zhangjiakou city are 54.0%–64.7% (water erosion), 26.6%–45.2% (wind erosion) (Table 2). The fraction of land area experiencing erosion intensity 2–25 t ha^{-1} yr^{-1} are 33.3%–43.8% (water erosion), 54.8%–63.5% (wind erosion). Our calculations suggest that greater than 80% of the land area in Zhangjiakou city has soil erosion rates of less than 25 t ha^{-1} yr^{-1}. The region has erosion hot spots, however. In particular, we predict minimal water erosion intensity <2 t ha^{-1} yr^{-1} as the dominant intensity category, whereas the erosion intensity of 2–25 t ha^{-1} yr^{-1} is dominant for wind erosion. This, to some extent, explains the difference of average erosion rate between water and wind erosion. We aim to explain this discrepancy and explore how it correlates with soil quality measurements.

The spatial distribution of soil erosion intensities are similar for the years 2005, 2010 and 2015 (Fig. 4). Compared to other regions, wind erosion rates are higher in the northwest region and southeast corner of Zhangjiakou city. In the northwest region, the wind erosion rates reach 8.7–15.7 t ha^{-1} yr^{-1} over the three years, whereas the wind erosion rates in southwest region account for 2.7–4.4 t ha^{-1} yr^{-1}. Calculations of water erosion stand in contrast to wind erosion: they have larger values in southwestern Zhangjiakou city, displaying a banded pattern from southwest to northeast (Fig. 4). In the southwestern Zhangjiakou city, water erosion rates reach 4.2–4.4 t ha^{-1} yr^{-1} over the three studies years, the value in northwest region accounts for 2.3–4.3 t ha^{-1} yr^{-1}.

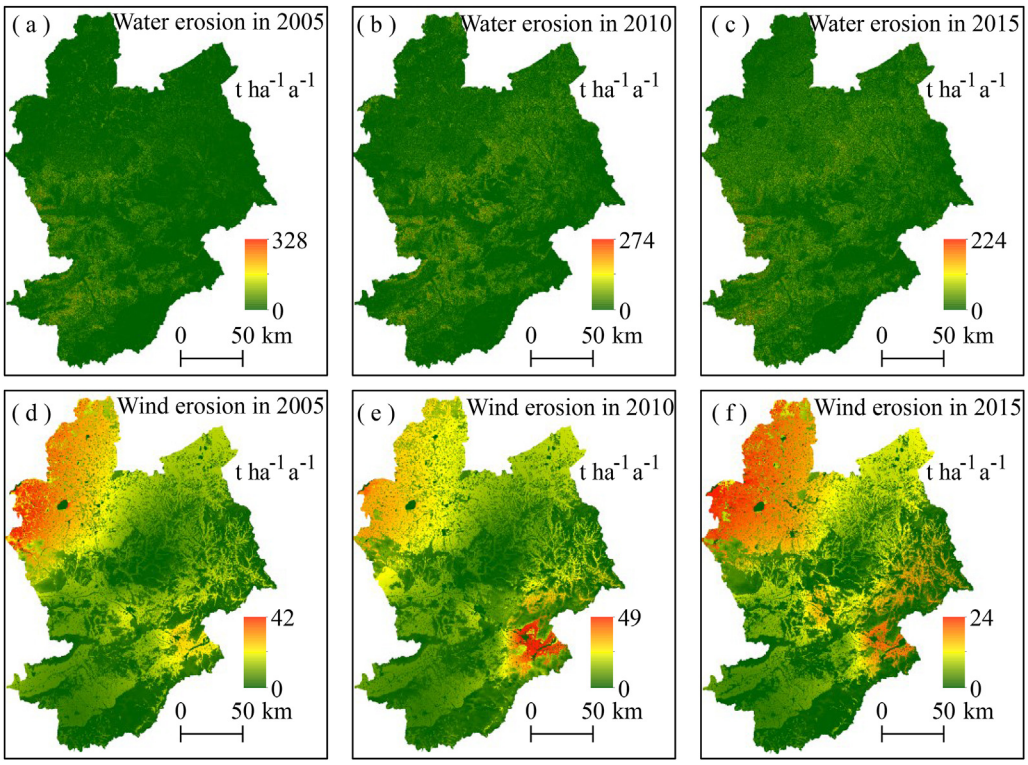

Fig. 4. The spatial distribution of water and wind erosion in Zhangjiakou city.

3.2. Total erosion derived from the models and from ^{137}Cs inventories

Using the logarithmic regression formula between soil erosion and ^{137}Cs inventory (collected in 2008), the average soil erosion rate in southeast Zhangjiakou city was calculated to be 16.7 t ha^{-1} yr^{-1}. In the same area, the average value of modelled total erosion rates were 7.4,15.3 and 7.2 t ha^{-1} yr^{-1} for the year 2005, 2010 and 2015, respectively. In general, the erosion rate derived from ^{137}Cs is of the same order of magnitude as modelled erosion rates, and is closes to the estimated total erosion rate of 15.3 t ha^{-1} yr^{-1} in 2010. Meanwhile, the spatial distribution of total erosion in southeastern Zhangjiakou city inferred from ^{137}Cs inventories is similar to that of the modelled erosion rates in 2010: both predict a hotspot of erosion in the southeastern corner of Zhangjiakou city (Fig. 5).

Fig. 5 shows that the modelled total erosion in the whole area of Zhangjiakou city presents a spatial pattern with relatively high erosion rates in northwest and southeast regions of Zhangjiakou city. The spatial pattern of total erosion for each year is similar to that of wind erosion in Zhangjiakou city (Fig. 4) because wind erosion dominates the total erosion signal compared to water erosion.

3.3. Relations between soil erosion and soil quality

The proportion of the grain size distribution greater than 0.099 mm, and soil saturated hydraulic conductivity (K_s), and the total N content are positively correlated with modelled wind and total erosion (Fig. 6). In contrast, the field capacity of soil water is negatively correlated with wind and total erosion (Fig. 6). However, for some soil quality parameters the direction of correlation differs between water and wind erosion. Total erosion follows the same pattern as wind erosion because, as previously stated, wind erosion dominates the total erosion across the study area. Water erosion has a positive relationship with the content of SOC, and a negative relationship with soil saturated hydraulic conductivity (K_s). Moreover, the regression coefficient, R^2, between wind erosion and soil quality parameters range from 0.57 to 0.85, and correlation coefficients are higher than that between water erosion and soil quality parameters, as well as between total erosion and soil quality parameters.

We found that the relationships between soil erosion and soil quality in arable land and in non-arable land are similar to that in the whole study area (Fig. 7). The correlation between soil particle size and water erosion, and the correlation between Ks and total erosion are significant in arable land, however, these two correlations are not significant in non-arable land ($P < 0.01$), indicates that the relationships between soil erosion and soil quality in arable land are more reliable than them in non-arable land. In addition, among five soil quality parameters, four parameters have significant correlation with wind erosion ($P < 0.01$), while three parameters and two parameters significantly correlate with water erosion and total erosion, respectively ($P < 0.01$).

4. Discussion

4.1. The influence factors on soil erosion

Zhang et al. (2018) claimed that climate variation was the dominant factor controlling changes in wind erosion, as it drives changes in wind speeds. The dominant wind direction over Zhangjiakou city is from the northwest to the southeast. Driving the patterns in wind erosion is physiography. The distribution of blown sand and dust events in 2015 shows that the cumulative duration of blown sand and dust events in northern Zhangjiakou city are much higher than other regions (Fig. 8). The distribution pattern of blown sand and dust events is similar to that of wind erosion. However, rainfall-runoff erosivity factor (R) in 2015 exhibits high values in the

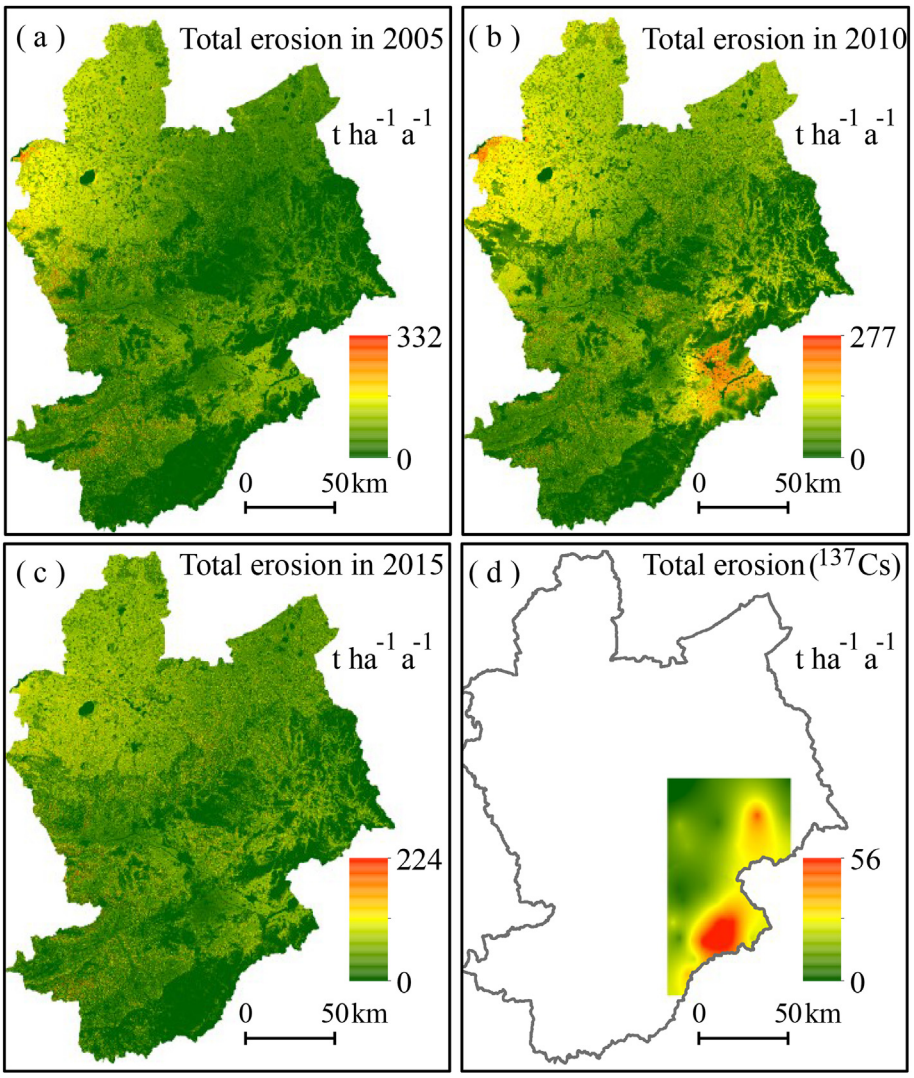

Fig. 5. The spatial distribution of total erosion in Zhangjiakou city.

east region of Zhangjiakou city, and the distribution pattern is different from that of water erosion (Fig. 8), implies that the distribution of water erosion would be more affected by other factors such as landscape, land use and plant cover, rather than mostly affected by the rainfall-runoff erosivity factor.

From the perspective of landscape, we found that high water erosion rates mainly occur at elevations between 800 and 1300 m (Table 3), which are the elevations that represent a transition zone between the Inner Mongolia Plateau and North China Plains. Water erosion rates are also high at slopes of 5°–15°, grassland and arable land, and areas with plant coverage 10–30%. High wind erosion rates mainly present at elevations <800 m (alluvial plain of Yanghe river and Sanggan river) and elevations between 1300 and 2000m (on the Inner Mongolian Plateau), slopes less than 15°and especially in very gentle areas with the slope less than 5°, arable land, and areas with plant coverage 10–30%.

Furthermore, we extracted the land area ratio of different land use types, as well as plant coverage in different topographic gradient grades. Fig. 9 shows that, arable land are primary land use types in slope grades 0–5° and 5–15°, with land area ratio of 68.9% and 46.4%, respectively. However, in slope grades 15–25° and >25°, forest and grass land are primary land use types. In addition, the plant coverage increase from 30.5% in slope grade 0–5° to 51.4% in slope grade >25°.These results above indicate that human activities which relate to farming and deforestation activities are the most important factors to decide the distribution of water and wind erosion. Topographic gradient might still be driving the pattern of soil erosion, but indirectly as it determines the land use pattern and plant coverage around Zhangjiakou city.

4.2. Spatial scale effect on the relations between soil erosion and soil quality

It is commonly thought that soil erosion creates distinct spatial variations in soil quality. However, soil erosion is a scale-dependent phenomenon, and the different spatial scale effects on soil quality can vary widely (Berhe et al., 2018). At the small spatial scale, such as the hillslope scale, soil erosion process and other factors that influence soil quality such as topography and land use type, are relatively homogeneous, and the effects of soil erosion on the soil quality distribution would be more significant (Visser & Sterk, 2007). At the regional scale, the factors that influence the soil quality distribution are various and heterogeneous, and so they may weaken the relations between soil erosion and soil quality.

In this study, we found that grain size fraction >0.099 mm, field capacity of soil water, and total nitrogen (N) do not have significant

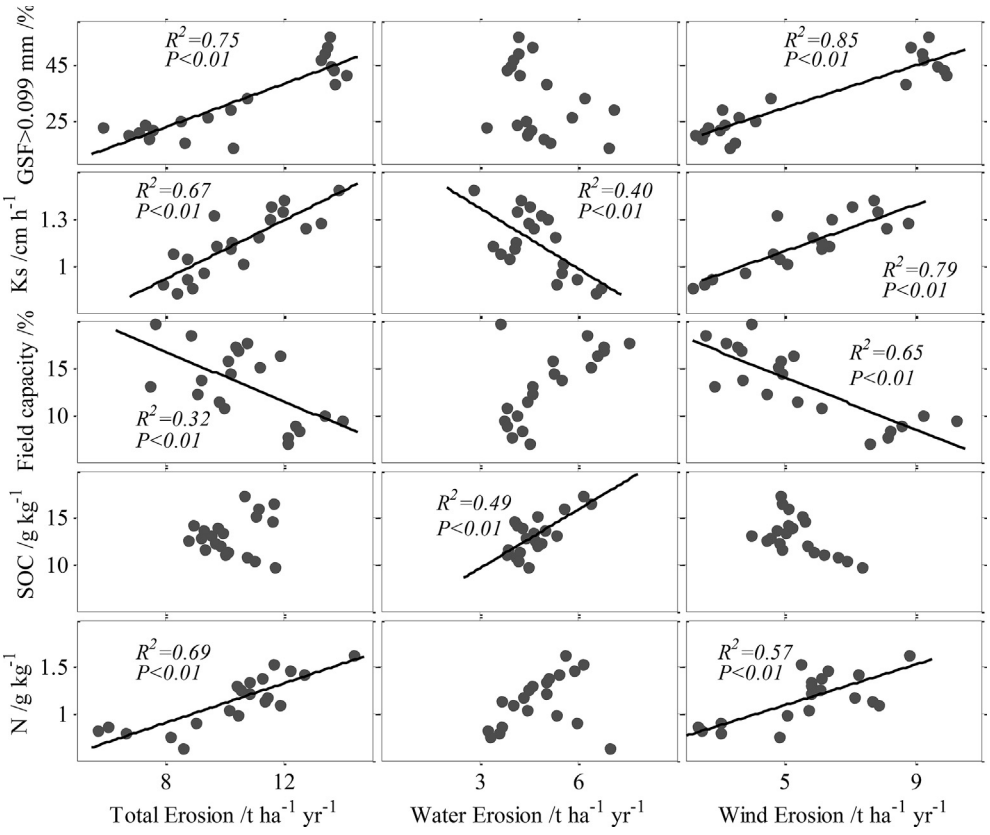

Fig. 6. The relationship between soil erosion and soil quality.

correlations with water erosion, and SOC does not have significant correlation with wind erosion ($P < 0.01$). In addition, different soil erosion mechanisms at the regional scale may have a distinct spatial distribution, their influence on the distribution of soil quality could interact to each other, thus increase the uncertainty of single soil erosion impact on soil quality at the regional scale. In this study, we found that the correlation direction may differs between water and wind erosion. We also found because wind erosion in Zhangjiakou city dominates the total erosion across the study area, total erosion in simple linear regressions follow the same pattern as wind erosion.

Therefore, our observed relationships between soil quality and soil erosion may be a function of the spatial scales of observation, with some relationships potentially due to the small scale or in-situ observation, and we may not be capturing these relationships at regional spatial scales.

4.3. Soil erosion and soil degradation

In this study, the proportion of the grain size fraction >0.099 mm has a positive correlation with wind and total erosion ($P < 0.01$), which is consistent with predicted coarsening of the soil surface by aeolian winnowing. Li, Okin, and Epstein (2009b) has reported that soil particles in the fractions of <0.125 mm were significantly depleted after wind erosion seasons. Yan et al. (2013) also found that the most reduction occurs between grain sizes of 0.05–0.09 mm after wind erosion experiments. In this study, the relationship between soil erosion and the change in soil grain size in surface soil is consistent with previous studies.

Soil saturated hydraulic conductivity (K_s) and field capacity of soil water not only are important parameters to assess the effect of soil and water conservation but also are key factors to affect the soil hydrological process (Duan et al., 2018). K_s reflects the water infiltration and determines water distribution (Wang et al., 2018a). In this study, K_s has a positive relation with wind and total erosion, but a negative relation with water erosion. We hypothesize that this is because the surface soil becomes coarser with accelerated wind erosion, leading to greater porosity and water infiltration rates (Duan et al., 2018; Zhang, Chan, Oates, Heenan, & Huang, 2007b). In addition, severe wind erosion rates occur in northern Zhangjiakou city where there is relatively low water erosion (Fig. 4). This causes a negative relationship between water erosion and K_s at the regional scales. Furthermore, increasing water infiltration in severe wind erosion region would weaken the water erosion process by decreasing runoff, thus, larger water infiltration also leads to lower water erosion intensity (Ruiz-Colmenero, Bienes, Eldridge, & Marques, 2013; Zhang et al., 2007b). Therefore, the difference between spatial distributions of wind erosion and water erosion may enhance negative relation between water erosion and K_s at the regional scale. The field capacity of soil water has a negative correlation with wind and total erosion, indicating that the soil water holding capacity becomes greater with slower rates of wind erosion.

Soil organic carbon (SOC) and nitrogen (N) are two important nutrients related to biogeochemical cycling (Quinton, Govers, Van Oost, & Bardgett, 2010). Previous studies argued that SOC and N were preferentially removed by water and wind erosion (Lal, 2018). The loss of SOC and N have positive relationships with soil erosion intensity (Yan, Wang, Wang, Zhang, & Patel, 2005, 2013), and SOC and N contents in the residue soil have a negative relationship with soil erosion intensity (Su et al., 2017; Zou et al., 2018). However, a recent study argued that SOC content in sediments are minimally affected by the amount of soil loss because of soil zonality which relates to how the soils formation and evolve (Li et al., 2017c). Li

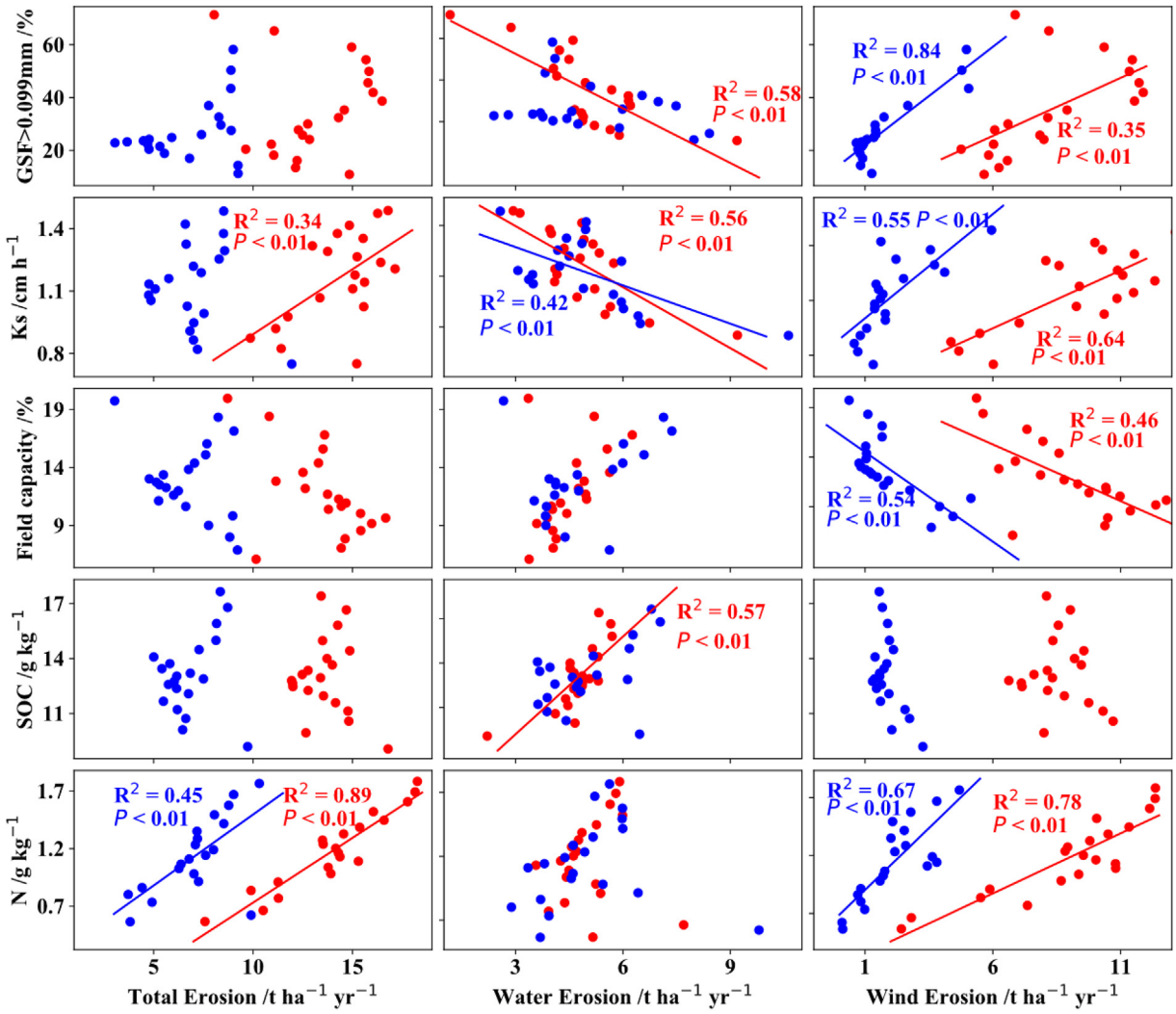

Fig. 7. The relationship between soil erosion and soil quality for arable land and non-arable land, respectively.

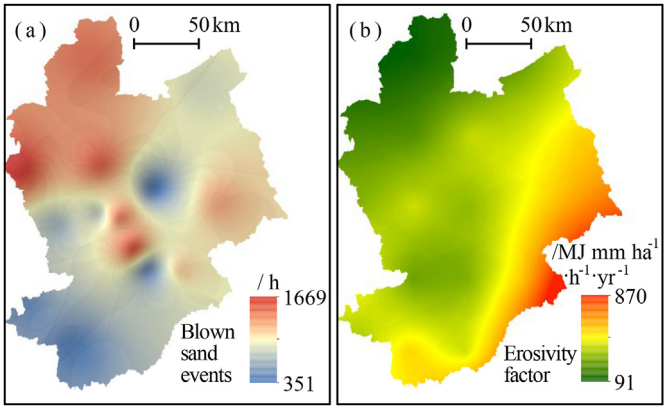

Fig. 8. The rainfall-runoff erosivity factor and cumulative duration of blown sand and dust events in Zhangjiakou city.

et al. (2017b) reported that the contents of SOC and total N have no significant correlation with soil erosion in artificial grassland in semiarid China. In addition, Parfitt et al. (2013) found that gains in soil carbon and nitrogen under hill country pasture are probably largely due to the ongoing input from carbon and nitrogen in the grass-legume pastures rather than erosion or depositional of soil. Therefore, the relations between soil erosion and soil nutrient (SOC and N) may not follow the negative rule due to different processes of soil nutrient input. In this study, the content of SOC has a positive relationship with water erosion ($P < 0.01$) (Fig. 6). Severe water erosion in Zhangjiakou city occurs in the southwest and central regions (Fig. 4) where surface soil particles are finer compared to areas with severe wind erosion rates: fine particles in soil are conducive to increase SOC contents (e.g., Doetterl et al., 2016; Eusterhues, Rumpel, & Kogel-Knabner, 2005; Wang et al., 2018b). In addition, both plants and erosion may play an important role in redistributing soil nutrients (Eger et al., 2018; Li, Zhao, Liu, & Huang, 2009a). We found severe water erosion in Zhangjiakou city occur in grass land as well as areas with vegetation (30–50%) (Table 3), the plant material that is either emplaced by roots or dropped and buried within the sediment would enrich the content of SOC.

In our case, the total N content is positively correlated with wind and total erosion. Severe wind erosion occurs in arable land and regions with lower vegetation coverage (10–30%) (Table 3). The total N were mainly concentrated in the uppermost soil layer (0–10 cm) in a semiarid region (Li et al., 2017a). Hence, soil erosion

Table 3
Water and wind erosion intensity within different influencing factors.

		Water erosion			Wind erosion		
		2005	2010	2015	2005	2010	2015
Elevation/m	<800	2.7 ± 5.1	3.0 ± 6.0	2.5 ± 4.9	**7.9 ± 5.9**	**14.1 ± 14.2**	**5.4 ± 5.1**
	800–1300	**4.9 ± 9.1**	**5.3 ± 9.0**	**5.1 ± 8.5**	5.1 ± 5.4	7.7 ± 8.0	3.4 ± 4.1
	1300–2000	2.4 ± 5.1	3.9 ± 6.5	4.4 ± 7.0	**9.3 ± 8.8**	**11.3 ± 9.7**	**6.2 ± 5.7**
	>2000	1.9 ± 2.6	3.3 ± 5.1	3.3 ± 6.0	0.8 ± 1.1	2.8 ± 2.2	0.7 ± 1.1
Slope/Degree	<5	2.6 ± 5.1	3.0 ± 5.1	3.2 ± 5.1	**10.8 ± 7.8**	**14.0 ± 10.5**	**7.2 ± 5.3**
	5–15	**5.0 ± 8.9**	**6.4 ± 9.5**	**6.8 ± 9.4**	7.8 ± 7.5	10.2 ± 9.2	5.2 ± 5.1
	15–25	2.6 ± 6.6	4.1 ± 7.7	3.8 ± 7.6	2.5 ± 3.8	4.5 ± 6.0	1.7 ± 3.0
	>25	1.0 ± 2.9	2.0 ± 3.9	1.8 ± 3.5	1.2 ± 2.0	3.0 ± 4.1	0.7 ± 1.7
Land use/%	Forest	0.3 ± 1.5	0.6 ± 1.9	2.2 ± 5.1	1.6 ± 2.8	3.4 ± 3.4	1.0 ± 1.7
	Grass	**5.5 ± 9.9**	**7.8 ± 10.9**	**6.3 ± 10.0**	3.0 ± 4.2	3.9 ± 4.3	1.8 ± 2.6
	Arable	2.8 ± 5.6	3.9 ± 5.9	4.4 ± 6.7	**12.2 ± 7.3**	**16.8 ± 9.2**	**9.0 ± 4.5**
	Other	2.3 ± 6.4	2.3 ± 6.8	1.3 ± 4.1	5.4 ± 7.7	6.7 ± 10.4	3.0 ± 5.3
Plant coverage/%	<10	1.3 ± 5.2	2.1 ± 8.9	0.4 ± 1.9	6.0 ± 13.5	6.5 ± 14.4	2.0 ± 6.3
	10–30	**4.4 ± 8.2**	**4.7 ± 8.4**	**5.0 ± 8.1**	**10.3 ± 8.0**	**13.7 ± 10.0**	**8.0 ± 5.9**
	30–50	**1.9 ± 3.9**	**4.8 ± 7.5**	**5.0 ± 7.7**	3.5 ± 4.4	9.7 ± 9.5	4.3 ± 4.3
	>50	0.2 ± 0.6	0.9 ± 2.3	1.5 ± 3.1	0.7 ± 1.3	2.7 ± 4.5	0.7 ± 2.0

The unit of water and wind erosion intensity is: t ha^{-1} yr^{-1}.

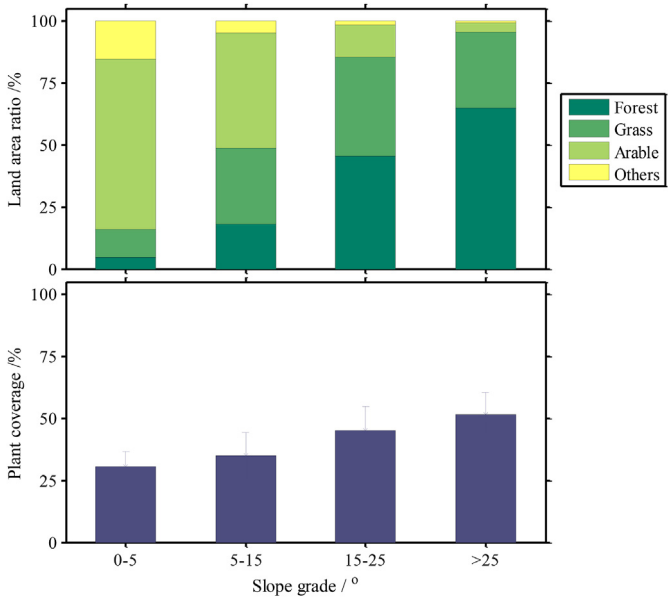

Fig. 9. Land use types and plant coverage in different slope grades.

could lead to the mixing of carbon-poor or nutrient-poor subsoil into the layer mixed by tillage, and if the newly exposed mineral surfaces bind organic matter, soil carbon and nutrient inventories may also increase (Quinton et al., 2010). In northern Zhangjiakou city with severe wind erosion intensity, total N could be lost from bare unprotected soils towards areas with sufficient vegetation or mulch cover because of wind erosion process at the local scale. However, in a balance between deposition on fields and denudation from fallow areas, and the long-term N import or export due to wind erosion on the scale of a village or cluster of farms can be assumed zero (Visser & Sterk, 2007). In addition, we predict a low intensity of wind erosion in the southwest region of Zhangjiakou city (Fig. 4), but this area exhibits higher than average water erosion. Nutrients transported by water are always directed in a down-slope direction and cannot be transported upslope again as is possible with wind erosion. Total N lost by water erosion are forever lost for the upslope area (Visser & Sterk, 2007). Thus, these mechanism above would explain the positive relationship between wind erosion and soil nutrient at the regional scale.

Overall, the relationship between soil quality and soil erosion varies on regional scales, and the correlations between them, can be caused by many different processes: i.e., we cannot make a definitive causal link between these two datasets. The data does show that, compared to water erosion, wind erosion displays higher correlation coefficients with soil quality parameters in Zhangjiakou city possibly because of its dominance compared to water erosion in contributing to total erosion.

5. Conclusion

In this study, we calculated annual soil erosion rates using USLE and a wind erosion model, as well as calculated long-term soil erosion rates in decade scale based on ^{137}Cs inventories, to assess the spatial distribution of soil erosion intensity and its influence on soil degradation in Zhangjiakou city.

We find that soil erosion rates in Zhangjiakou city in the decade before 2015 were 2.92–4.14 t ha^{-1} yr^{-1} for water erosion and 4.99–10.05 t ha^{-1} yr^{-1} for wind erosion. More than 80% of the land area in the Zhangjiakou city region are eroding at less than 25 t ha^{-1} yr^{-1}. Areas with higher potential wind and total erosion risk occur mainly in northwest and southeast Zhangjiakou city, whereas potential water erosion risk is highest in the southwest and central regions. The spatial distribution of total erosion rates in decade scale, which calculated based on ^{137}Cs inventories, is similar to the spatial distribution of annual soil erosion in 2005, 2010 and 2015.

Higher soil erosion intensities in Zhangjiakou city occur primarily in areas with gentle slope, lower plant coverage and areas of arable land. Topographic slope plays an important role in determining erosion rates, but in an indirect fashion. Areas with high topographic slopes have not been used for farming, and are primarily forested. In the Zhangjiakou city region, the dominant erosion mechanism is wind erosion, driven by low plant cover on fallow fields, and so human modification of the landscape, partially determined by topographic gradient, is the primary driver of soil erosion in Zhangjiakou city.

We find complex relationships between soil erosion and soil quality parameters in Zhangjiakou city. However, some clear trends do emerge. Surface soil becomes coarser and water infiltration is enhanced as wind erosion is greater, whereas the soil water holding capacity decreases with increasing wind erosion rates. However, in regions with higher water infiltration rates, the intensity of water erosion is lower. The relations between the distributions of soil

nutrient and soil erosion present positive patterns, which are varied, and likely caused by a suite of different processes. Our analysis of the relationships of soil nutrient parameters with soil erosion may be a function of the spatial scales of observation. Meanwhile, compared to water erosion, wind erosion has more significant correlations with soil quality in Zhangjiakou city possibly because of its dominance compared to water erosion in contributing to total erosion. To mitigate risks of soil degradation, suitable erosion measures should be implemented according to the dominant erosion type, which varies in space. The measures will protect the regional environment in advance of the 2022 Winter Olympics.

Acknowledgments

This work was supported by National Major Science and Technology Program for Water Pollution Control and Treatment (2017ZX07101001) of China; Scientific and Technological Research Program of Chongqing Municipal Education Commission (KJ110608) of China, and the Chinese Government Scholarship from China Scholarship Council (CSC). We would like to thank National Earth System Science Data Center, National Science & Technology Infrastructure of China (http://www.geodata.cn), the National Meteorological Information Center of China (http://data.cma.cn), the Geospatial Data Cloud website (http://www.gscloud.cn) , and the Data Center for Resources and Environmental Sciences, Chinese Academy of Science (RESDC) to give us data support including the daily meteorological data, NDVI, DEM, and the land use dataset. We thank Dr. Wu Yongqiu and Dr. Zhang Chunlai at the Beijing Normal University for their assistance with soil erosion calculation. We thank Dr. Wei Jie and Li Shasha at the Chongqing Normal University for their assistance during the field work. We also acknowledge Dr. Liu Muxing and Dr. Yi Jun and Lou Shulan at the Central China Normal University, as well as Dr. Wang Yong and Liu Chuan at the Southwest University for their assistance with measurements of soil parameters.

References

Aksoy, H., & Kavvas, M. L. (2005). A review of hillslope and watershed scale erosion and sediment transport models. *Catena, 64*, 247–271. https://doi.org/10.1016/j.catena.2005.08.008.

Berhe, A. A., Barnes, R. T., Six, J., & Marín-Spiotta, E. (2018). Role of soil erosion in biogeochemical cycling of essential elements: Carbon, nitrogen, and phosphorus. *Annual Review of Earth and Planetary Sciences, 46*, 521–548. https://doi.org/10.1146/annurev-earth-082517-010018.

Bilotta, G. S., Grove, M., & Mudd, S. M. (2012). Assessing the significance of soil erosion: Boundary Crossings. *Transactions of the Institute of British Geographers, 37*, 342–345. https://doi.org/10.1111/j.1475-5661.2011.00497.x.

Breshears, D. D., Whicker, J. J., Johansen, M. P., & Pinder, J. E. (2003). Wind and water erosion and transport in semi-arid shrubland, grassland and forest ecosystems: Quantifying dominance of horizontal wind-driven transport. *Earth Surface Processes and Landforms, 28*, 1189–1209. https://doi.org/10.1002/esp.1034.

Cyranoski, D. (2015). Chinese biologists lead Olympics outcry. *Nature, 524*, 278–279.

Doetterl, S., Berhe, A. A., Nadeu, E., Wang, Z., Sommer, M., & Fiener, P. (2016). Erosion, deposition and soil carbon: A review of process-level controls, experimental tools and models to address C cycling in dynamic landscapes. *Earth-Science Reviews, 154*, 102–122. https://doi.org/10.1016/j.earscirev.2015.12.005.

Duan, X., Deng, Y., Tao, Y., He, Y., Lin, L., & Chen, J. (2018). Variation in soil saturated hydraulic conductivity along the hillslope of collapsing granite gullies. *Hydrological Sciences Journal, 63*, 803–817. https://doi.org/10.1080/02626667.2018.1453610.

Du, H., Dou, S., Deng, X., Xue, X., & Wang, T. (2016). Assessment of wind and water erosion risk in the watershed of the Ningxia-Inner Mongolia Reach of the Yellow River, China. *Ecological Indicators, 67*, 117–131. https://doi.org/10.1016/j.ecolind.2016.02.042.

Efthimiou, N. (2018). The importance of soil data availability on erosion modeling. *Catena, 165*, 551–566. https://doi.org/10.1016/j.catena.2018.03.002.

Eger, A., Yoo, K., Almond, P. C., Boitt, G., Larsen, I. J., Condron, L. M., et al. (2018). Does soil erosion rejuvenate the soil phosphorus inventory? *Geoderma, 332*, 45–59. https://doi.org/10.1016/j.geoderma.2018.06.021.

Eusterhues, K., Rumpel, C., & Kogel-Knabner, I. (2005). Organo-mineral associations in sandy acid forest soils: Importance of specific surface area, iron oxides and micropores. *European Journal of Soil Science, 56*, 753–763. https://doi.org/10.1111/j.1365-2389.2005.00710.x, 0, 050912034650049.

Fu, B., Liu, Y., Lü, Y., He, C., Zeng, Y., & Wu, B. (2011). Assessing the soil erosion control service of ecosystems change in the Loess Plateau of China. *Ecological Complexity, 8*, 284–293. https://doi.org/10.1016/j.ecocom.2011.07.003.

Gao, S., Zhang, C., Zou, X., Wu, Y., Wei, X., Huang, Y., et al. (2012). *Benefits of Beijing-Tianjin sand source control engineering*. Beijing: China Science Publishing & Media Ltd (in Chinese).

Jiang, Z., Wang, Z., & Liu, Z. (1996). Quantitative study on spatial variation of soil erosion in a small watershed in the Loess Hilly Region. *Journal of Soil Erosion and Soil Conservation, 2*, 1–9 (in Chinese).

Jiang, C., Zhang, H., Zhang, Z., & Wang, D. (2019). Model-based assessment soil loss by wind and water erosion in China's Loess Plateau: Dynamic change, conservation effectiveness, and strategies for sustainable restoration. *Global and Planetary Change, 172*, 396–413. https://doi.org/10.1016/j.gloplacha.2018.11.002.

Lal, R. (2001). Soil degradation by erosion. *Land Degradation & Development, 12*, 519–539. https://doi.org/10.1002/ldr.472.

Lal, R. (2018). Accelerated Soil erosion as a source of atmospheric CO_2. In *Soil and tillage Research*. https://doi.org/10.1016/j.still.2018.02.001.

Li, D., Fan, J., Zhang, X., Xu, X., He, N., Wen, X., et al. (2017a). Hydrolase kinetics to detect temperature-related changes in the rates of soil organic matter decomposition. *European Journal of Soil Biology, 81*, 108–115. https://doi.org/10.1016/j.ejsobi.2016.10.004.

Li, M., Li, Z., Liu, P., & Yao, W. (2005). Using cesium-137 technique to study the characteristics of different aspect of soil erosion in the wind-water erosion crisscross region on Loess Plateau of China. *Applied Radiation and Isotopes, 62*, 109–113. https://doi.org/10.1016/j.apradiso.2004.06.005.

Li, Z., Liu, C., Dong, Y., Chang, X., Nie, X., Liu, L., et al. (2017b). Response of soil organic carbon and nitrogen stocks to soil erosion and land use types in the Loess hilly–gully region of China. *Soil and Tillage Research, 166*, 1–9. https://doi.org/10.1016/j. still.2016.10.004.

Li, Z., Nie, X., He, J., Chang, X., Liu, C., Liu, L., et al. (2017c). Zonal characteristics of sediment-bound organic carbon loss during water erosion: A case study of four typical loess soils in shaanxi province. *Catena, 156*, 393–400. https://doi.org/10.1016/j.catena.2017.05.001.

Li, J., Okin, G. S., & Epstein, H. E. (2009b). Effects of enhanced wind erosion on surface soil texture and characteristics of windblown sediments. *Journal of Geophysical Research: Biogeosciences, 114*, G02003. https://doi.org/10.1029/2008JG000903.

Liu, B., Bi, X., & Fu, S. (2010). *Beijing soil loss equation*. Beijing: China Science Publishing & Media Ltd (in Chinese).

Liu, R., Liu, J., Zhang, Z., Borthwick, A. G. L., Cai, Y., Dong, L., et al. (2018). Risks of airborne pollution accidents in a major conurbation: Case study of Zhangjiakou, a host city for the 2022 winter Olympics. *Stochastic Environmental Research and Risk Assessment, 32*, 3257–3272. https://doi.org/10.1007/s00477-018-1590-5.

Liu, B., Nearing, M. A., & Risse, L. M. (1994). Slope gradient effects on soil loss for steep slopes. *Transactions of the ASAE, 37*, 1835–1840.

Li, F., Zhao, W., Liu, J., & Huang, Z. (2009a). Degraded vegetation and wind erosion influence soil carbon, nitrogen and phosphorus accumulation in sandy grasslands. *Plant and Soil, 317*, 79–92. https://doi.org/10.1007/s11104-008-9789-8.

Nearing, M. A., Xie, Y., Liu, B., & Ye, Y. (2017). Natural and anthropogenic rates of soil erosion. *International Soil and Water Conservation Research, 5*, 77–84. https://doi.org/10.1016/j.iswcr.2017.04.001.

Parfitt, R. L., Baisden, W. T., Ross, C. W., Rosser, B. J., Schipper, L. A., & Barry, B. (2013). Influence of erosion and deposition on carbon and nitrogen accumulation in resampled steepland soils under pasture in New Zealand. *Geoderma, 192*, 154–159. https://doi.org/10.1016/j.geo derma.2012.08.006.

Qi, Y., Liu, J., Shi, H., Hu, Y., & Zhuang, D. (2008). Using 137Cs tracing technique to estimate wind erosion rates in the typical steppe region, northern Mongolian Plateau. *Science Bulletin, 53*, 1423–1430. https://doi.org/10.1007/s11434-008-0070-6.

Quinton, J. N., Govers, G., Van Oost, K., & Bardgett, R. D. (2010). The impact of agricultural soil erosion on biogeochemical cycling. *Nature Geoscience, 3*, 311–314. https://doi.org/10.1038/ngeo838.

Renard, K. G., & USA, U. S. A. (Eds.). (1997). *Predicting soil erosion by water: A guide to conservation planning with the revised universal soil loss equation (RUSLE)*. Washington, DC: Agriculture handbook.

Ruiz-Colmenero, M., Bienes, R., Eldridge, D. J., & Marques, M. J. (2013). Vegetation cover reduces erosion and enhances soil organic carbon in a vineyard in the central Spain. *Catena, 104*, 153–160. https://doi.org/10.1016/j.catena.2012.11.007.

Shi, P., Yan, P., Yuan, Y., & Nearing, M. A. (2004). Wind erosion research in China: Past, present and future. *Progress in Physical Geography: Earth and Environment, 28*, 366–386. https://doi.org/10.1191/0309133304pp416ra.

Song, S., Zhang, S., Wang, T., Meng, J., Zhou, Y., & Zhang, H. (2018). Balancing conservation and development in winter olympic construction: Evidence from a multi-scale ecological suitability assessment. *Scientific Reports, 8*. https://doi.org/10.1038/s41598-018-32548-2.

Su, Z., Li, Y., Zhang, J., Xiong, D., Dong, Y., Zhang, S., et al. (2017). Spatial variation in soil, SOC, and total N redistribution on affected and non-affected slope terraces due to the 8.0 Wenchuan Earthquake in 2008 by using 137 Cs technique. *Catena, 155*, 191–199. https://doi.org/10.1016/j.catena.2017.03.018.

Teng, H., Liang, Z., Chen, S., Liu, Y., Viscarra Rossel, R. A., Chappell, A., et al. (2018). Current and future assessments of soil erosion by water on the Tibetan Plateau based on RUSLE and CMIP5 climate models. *The Science of the Total Environment, 635*, 673–686. https://doi.org/10.1016/j.scitotenv.2018.04.146.

Tuo, D., Xu, M., & Gao, G. (2018). Relative contributions of wind and water erosion to total soil loss and its effect on soil properties in sloping croplands of the Chinese

Loess Plateau. *The Science of the Total Environment, 633*, 1032–1040. https://doi.org/10.1016/j.scitotenv.2018.03. 237.
Tuo, D., Xu, M., Zhao, Y., & Gao, L. (2015). Interactions between wind and water erosion change sediment yield and particle distribution under simulated conditions. *Journal of Arid Land, 7*, 590–598. https://doi.org/10.1007/s40333-015-0128-7.
Van Pelt, R. S., Hushmurodov, S. X., Baumhardt, R. L., Chappell, A., Nearing, M. A., Polyakov, V. O., et al. (2017). The reduction of partitioned wind and water erosion by conservation agriculture. *Catena, 148*, 160–167. https://doi.org/10.1016/j.catena.2016.07.004.
Visser, S. M., & Sterk, G. (2007). Nutrient dynamics—wind and water erosion at the village scale in the Sahel. *Land Degradation & Development, 18*, 578–588. https://doi.org/10.1002/ldr.800.
Visser, S. M., Sterk, G., & Ribolzi, O. (2004). Techniques for simultaneous quantification of wind and water erosion in semi-arid regions. *Journal of Arid Environments, 59*, 699–717. https://doi.org/10.1016/j.jaridenv.2004.02.005.
Visser, S. M., Stroosnijder, L., & Chardon, W. J. (2005). Nutrient losses by wind and water, measurements and modelling. *Catena, 63*, 1–22. https://doi.org/10.1016/j.catena.2005. 07.003.
Wang, Y., Shao, M., Han, X., & Liu, Z. (2015). Spatial variability of soil parameters of the van Genuchten model at a regional scale: Spatial variability of soil parameters of the van Genuchten model. *Clean - Soil, Air, Water, 43*, 271–278. https://doi.org/10.1002/clen. 201300903.
Wang, W., Wang, Y., Sun, Q., Zhang, M., Qiang, Y., & Liu, M. (2018a). Spatial variation of saturated hydraulic conductivity of a loess slope in the South Jingyang Plateau, China. *Engineering Geology, 236*, 70–78. https://doi.org/10.1016/j.enggeo.2017.08.002.
Wang, Y., Wu, Y., Lu, R., & Pan, M. (2018c). Application of Empirical Orthogonal Function (EOF) method to detect the spatial grain-size fractionation of aeolian sediment and comparison with other methods in case studies from northwestern China. *Physical Geography, 39*, 216–229. https://doi.org/10.1080/02723646.2017.1361777.
Wang, X., Yoo, K., Mudd, S. M., Weinman, B., Gutknecht, J., & Gabet, E. J. (2018b). Storage and export of soil carbon and mineral surface area along an erosional gradient in the Sierra Nevada, California. *Geoderma, 321*, 151–163. https://doi.org/10.1016/j.geoderma.2018.02. 008.
Wei, W., Chen, L., Fu, B., Lü, Y., & Gong, J. (2009). Responses of water erosion to rainfall extremes and vegetation types in a loess semiarid hilly area, NW China. *Hydrological Processes, 23*, 1780–1791. https://doi.org/10.1002/hyp.7294.
Wischmeier, W., & Smith, D. (1978). *Predicting rainfall erosion losses —a guide to conservation planning.* U.S. Department of Agriculture, Agriculture Handbook. No.537.
Wu, Y., Ouyang, W., Hao, Z., Lin, C., Liu, H., & Wang, Y. (2018). Assessment of soil erosion characteristics in response to temperature and precipitation in a freeze-thaw watershed. *Geoderma, 328*, 56–65. https://doi.org/10.1016/j.geoderma.2018.05.007.
Yan, P., Dong, G., Zhang, X., & Zhang, Y. (2000). Preliminary results of the study on wind erosion in the Qinghai-Tibetan Plateau using137Cs technique. *Chinese Science Bulletin, 45*, 1019–1025. https://doi.org/10.1007/BF02884984.
Yan, P., Dong, G., Zhang, X., & Zou, X. (2003). Application of caesium-137 technique on wind erosion in gonghe basin, qinghai province. *Journal of Desert Research, 23*, 268–275 (in Chinese).
Yan, H., Wang, S., Wang, C., Zhang, G., & Patel, N. (2005). Losses of soil organic carbon under wind erosion in China. *Global Change Biology, 11*, 828–840. https://doi.org/10.1111/j.1365-2486.2005.00950.x.
Yan, Y., Xin, X., Xu, X., Wang, X., Yang, G., Yan, R., et al. (2013). Quantitative effects of wind erosion on the soil texture and soil nutrients under different vegetation coverage in a semiarid steppe of northern China. *Plant and Soil, 369*, 585–598. https://doi.org/10.1007/s11104-013-1606-3.
Yuan, J., Niu, Z., & Wang, C. (2006). Vegetation NPP distribution based on MODIS data and CASA model—a case study of northern Hebei Province. *Chinese Geographical Science, 16*, 334–341. https://doi.org/10.1007/s11769-006-0334-5.
Zhang, G., Chan, K., Oates, A., Heenan, D., & Huang, G. (2007b). Relationship between soil structure and runoff/soil loss after 24 years of conservation tillage. *Soil and Tillage Research, 92*, 122–128. https://doi.org/10.1016/j.still.2006.01.006.
Zhang, H., Fan, J., Cao, W., Harris, W., Li, Y., Chi, W., et al. (2018). Response of wind erosion dynamics to climate change and human activity in Inner Mongolia, China during 1990 to 2015. *The Science of the Total Environment, 639*, 1038–1050. https://doi.org/10.1016/j. scitotenv.2018.05.082.
Zhang, W., & Fu, J. (2003). Rainfall erosivity estimation under different rainfall amount. *Resources Science, 25*(1), 35–42 (in Chinese).
Zhang, Y., Nearing, M. A., Liu, B. Y., Van Pelt, R. S., Stone, J. J., Wei, H., et al. (2011b). Comparative rates of wind versus water erosion from a small semiarid watershed in southern Arizona, USA. *Aeolian Research, 3*, 197–204. https://doi.org/10.1016/j.aeolia. 2011.03.006.
Zhang, C., Yang, S., Pan, X., & Zhang, J. (2011a). Estimation of farmland soil wind erosion using RTK GPS measurements and the 137Cs technique: A case study in Kangbao county, Hebei province, northern China. *Soil and Tillage Research, 112*, 140–148. https://doi.org/10.1016/j.still.2010.12.003.
Zhang, J., Zhang, C., Chang, C., Wang, R., & Liu, G. (2017). Comparison of wind erosion based on measurements and SWEEP simulation: A case study in Kangbao county, Hebei province, China. *Soil and Tillage Research, 165*, 169–180. https://doi.org/10.1016/j.still.2016.08.006.
Zhang, C., Zou, X., Yang, P., Dong, Y., Li, S., Wei, X., et al. (2007a). Wind tunnel test and 137Cs tracing study on wind erosion of several soils in Tibet. *Soil and Tillage Research, 94*, 269–282. https://doi.org/10.1016/j.still.2006.08.002.
Zhao, J., Yang, Z., & Govers, G. (2019). Soil and water conservation measures reduce soil and water losses in China but not down to background levels: Evidence from erosion plot data. *Geoderma, 337*, 729–741. https://doi.org/10.1016/j.geoderma.2018.10.023.
Zhao, Y., Yan, D., Zhang, Q., Zhan, J., & Hu, H. (2012). Spatial distributions of 137Cs in surface soil in jing-jin-ji region, north China. *Journal of Environmental Radioactivity, 113*, 1–7. https://doi.org/10.1016/j.jenvrad.2012.04.005.
Zou, X., Li, J., Cheng, H., Wang, J., Zhang, C., Kang, L., et al. (2018). Spatial variation of topsoil features in soil wind erosion areas of northern China. *Catena, 167*, 429–439. https://doi.org/10.1016/j.catena.2018.05.022.